

# Forces Association-Based Active Contour

Aicha Baya Goumeidane, and Nafaa. Nacereddine

**Abstract**—A welded structure must be inspected to guarantee that the weld quality meets the design requirements to assure safety and reliability. However, X-ray image analyses and defect recognition with the computer vision techniques are very complex. Most difficulties lie in finding the small, irregular defects in poor contrast images which requires pre processing to image, extract, and classify features from strong background noise. This paper addresses the issue of designing methodology to extract defect from noisy background radiograph with image processing. Based on the use of actives contours this methodology seems to give good results

**Keywords**—Welding, Radiography, Computer vision, Active contour.

## I. INTRODUCTION

THE inspection of welds is a very important task for assuring safety and reliability in several industrial sectors. For this purpose Non-Destructive Testing (NDT) techniques have been employed to test a material for surface or internal flaws without destroying the welded components. Among the methods of NDT, radiography (X-rays or sometimes gamma rays) seems to be the most effective method and the experts are able to identify most types of defects in the images produced by this method. Some of the most common weld defects that can be identified in the radiographic images are the worm holes (worm-like cavities), slag inclusion (slag or other foreign matter entrapped during welding), linear porosity (linear cavities due to entrapped gas), gas pores (spherical cavities due to entrapped gas), lack of fusion (lack of union between weld and parent metal) or crack (discontinuity by fracture in the metal).

The interpretation of weld radiographs even by experienced inspectors can, however, be subjective and time-consuming [1]. With the advances in information technology and artificial intelligence techniques, the opportunity arose to develop a radiographic inspection method capable of detecting and classifying welding defects automatically, minimizing the subjective evaluation errors inherent to the conventional method. That is why, several researchers have tried to automate the inspection process by employing image processing, pattern recognition and computer vision methods [2]. The goal of such methods is to give consistent, objective and reliable results. One of the essential processes in computer vision consists of reducing the huge quantity of information, contained in image of objects which we have to recognize, by

preserving only the most important points. For that purpose, image segmentation is applied to digitized radiography. It allows the initial separation of regions of interest into non-overlapping regions based on intensity or textural information. It is generally the first processing applied to the radiographs to detect defects [3]. Among the boundary extraction-based segmentation techniques, deformable model, also called active contours or snakes, are recognized to be one of the efficient tools for 2D/3D image segmentation. The active contour methods provide an effective way for segmentation, in which the boundaries of the objects are detected by evolving curves. Its success is based on strong mathematical properties and efficient numerical schemes. Since first introduced by Kass [4] in 1988, many efforts have been done on active contours, or snakes, for their application in image processing and computer vision, such as image segmentation. Since the introduction, active contour models have been widely used in image segmentation with promising results. The models are able to provide smooth and closed contours to recover object boundaries with subpixel accuracy, which is typically not possible in classical methods, such as edge detection and thresholding. The existing active contour models can be categorized into two classes: edge-based models [4–8] and region-based models [9–16].

In general, edge-based models typically use image gradient as an image-based force to attract the contour toward object boundaries. These models have been successfully used for general images with strong object boundaries, but they may suffer from boundary leakage problem. Hence they are adapted for a certain class of problems and fail in the presence of noise and weak gradient information along the boundaries [15][16]. Region-based models have better performance than edge-based models in the presence of weak boundaries. However, region-based models [8] tend to rely on intensity homogeneity and have exhibit better performance. Unfortunately the computational cost of such models is rather expensive due to the fact that the computations are made over a region.

This paper addresses the issue of extracting defects from radiographic images by following the different steps that we propose and the use of and hybrid active contour we develop in this work.

This paper is organized as follows: Section 2 will be used to relate some characteristics about the nature of the radiographic film images and describes the selection of the region of interest in radiograms. Moreover, it will be devoted the scheme used in the image pre processing. In section 3 we give a brief introduction to the mathematical formulation of the classical active contour including conventional snakes and GVF/GGVF snakes. In section 4 we present the hybrid

Aicha Baya Goumeidane is with the Welding and NDT Research Center, Chérâga, Algiers Algeria (phone : 213 21 36 18 50 ; fax: 213 21 36 18 50; e-mail: ab\_goumeidane@yahoo.fr).

Nafaa Nacereddine is with the Welding and NDT Research Center, Chérâga, Algiers Algeria (phone : 213 21 36 18 50 ; fax: 213 21 36 18 50; e-mail: nafaa.nacereddine@enp.edu.dz).

scheme we developed to create forces for the active contour. Section 5 is dedicated to experimental results. We draw the main conclusions in section 6.

## II. WELD DEFECT DATABASE, THE REGION OF INTEREST SELECTION AND PREPROCESSING

The radiographic films are often very dark and their density is rather large, therefore an ordinary scanner cannot give a sufficient lightening through a radiogram. Here, we have used a scanner AGFA Arcus II, (800 dpi, 256 grey levels). The radiographic films that we have digitized were extracted from the standard films provided by International Institute of Welding (IIW). After digitization, the principal characteristics of our images are:

1. Small contrast between the background and the weld defect regions. These last are characterized by unsharpened and blurred edges.
2. Pronounced granularity due to digitization and the type of film used in industrial radiographic testing.
3. Presence of background gradient of image characterizing the thickness variation of the irradiated component part.

For the reasons previously evoked, it becomes difficult, if not uncertain to detect, during the radiogram visualization, the presence of the small defects and to determine accurately their sizes. That is why, it is necessary to start with a pre-processing stage in order to reduce or eliminate the noise enclosing in the film and improve its visibility. This procedure permits to obtain an image which would facilitate later, to drive the snake model to the defects.

### A. ROI Selection

The first task in image pre-processing is the selection of the region of interest (ROI): the region where they suspect the presence of imperfections. The selection of the ROI saves the operator to make treatments on the useless parts of the image, permitting reduction of the computing time. The second advantage is to save the treatments based on the global approaches to use the irrelevant regions of the image, which can negatively influence the output results. In addition, the limitation of the image to a region of interest (ROI) prevents from the detection of false defects outside the weld [17].

### B. Noise Suppression and Contrast Enhancement

Since the parametric snake model is gradient information based, in case of a weak gradient field, these information are not strong enough to drive the snake model to the boundaries, and the model will perform poorly. On the other hand, in the presence of noise, the gradient information could attract the model to wrong edges. That is why a stage of noise suppression and contrast enhancement is necessary. The method we choose to eliminate the noise is image smoothing by an edge preserving diffusion procedure called anisotropic diffusion [18]. The advantage of the method is that homogenous regions are smoothed with a Gaussian kernel while the contours are preserved from attenuation. In view of the radiographic images characteristics, and to improve the

contrast quality and extract hidden defects, we select a set of adaptive contrast enhancement techniques based on mathematical morphology [19,20], image statistics [21,22], and adaptive histogram equalization [23] we applied to the images under investigation. The results are commented in section 5.

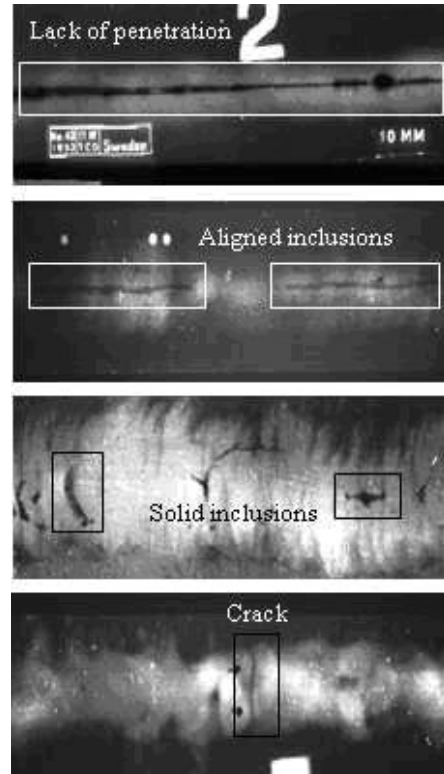


Fig. 1 Samples of Radiographic films and their associated ROIs

## III. MATH

The active contour method for image segmentation was introduced by Kass et al. in late 1980's. In this method, a curve represented by a chain points called the snake nodes, is evolved towards the object boundary under a force, until it stops at the boundary. More precisely, the curve moves to minimize the energy:

$$E(l) = \int_l \left( \frac{1}{2} (\alpha |l'(s)|^2 + \beta |l''(s)|^2) - \lambda |\nabla I(l(s))|^2 \right) ds \quad (1)$$

where  $l(s)$  represents the parameterized curve,  $I(x,y)$  is the image grey-level function, and constants  $\alpha, \beta, \lambda > 0$ . The first two terms in the energy functional smooth the curve. The third term attracts the curve to the object boundary, where the value of image gradient is large. The dynamics equation of the curve to minimize the total energy is given by

$$l_t(s) = \alpha l''(s) + \beta l'''(s) + \lambda \nabla |\nabla I(l(s))|^2 \quad (2)$$

The image function  $I(x,y)$  can be replaced by its smoothed version  $G_\sigma(x,y) * I(x,y)$ , where  $G_\sigma(x,y)$  is a two dimensional Gaussian function with zero mean and standard deviation  $\sigma$ , and the operator  $*$  is the convolution operator. Many efforts

have been made to improve this method. In [24,25], a constant force (pressure force) was added in the normal direction of the curve to accelerate its motion and increase the capture range. Eq.(3) represents the pressure force, where  $\vec{n}(s)$  is the normal unit vector to the curve at the point  $s$ ,  $k$  is a fixed scalar.

$$f(s) = k \cdot \vec{n}(s) \quad (3)$$

However the pressure force can not shrink and expand the balloon at different parts and hence his formulation leads to the fact that these forces must be initialized to push out or push in.

To solve the problem of these methods, Xu and Prince [6] proposed the gradient vector flow (GVF) method. Some modifications on this method were made afterwards [7]. In this method, the attractive force near the object boundary  $\nabla|\nabla I(l(s))|^2$  is extended to the whole computational region by diffusion. More precisely, they obtained a force field  $V = (u, v)$  from the image by minimizing the energy

$$E = \iint \mu(u_x^2 + u_y^2 + v_x^2 + v_y^2) + |\nabla f|^2 |V - \nabla f|^2 dx dy \quad (4)$$

where  $f = |\nabla I(x, y)|^2$ ,  $\nabla f = \nabla|\nabla I(x, y)|^2$  represents the attractive force to the boundary, and  $\mu$  is the diffusion constant. In this equation, near the object boundary,  $\nabla f$  is large, the second term dominates and the minimization gives  $V = \nabla f$ ; while away from the boundary,  $\nabla f$  is small and thus the second term is small, the energy is dominated by the diffusion term, which means that the force  $V$  is extended smoothly from its value near the object boundary. Therefore, the capture range is large and there is no need to place the initial curve entirely inside or outside the object.

Similar to equation (2) the dynamics equation of the curve to minimize the total energy can be expressed as:

$$l_t(s) = \alpha l''(s) + \beta l'(s) + V \quad (5)$$

However, the initial curve must still be placed near the object boundary to be detected, otherwise it might be attracted to a boundary of a wrong object or a wrong part of the boundary (see the image and the initial contour in the figure below).

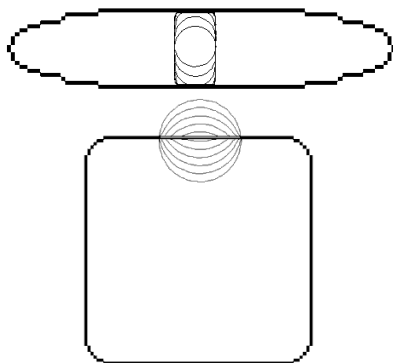


Fig. 2 GVF snake progression from an initialization to final contour for both GVF snakes

The explanation for such behavior came from the nature of the diffusion scheme of the GVF. Indeed the GVF snake must be initialized around the Centers of Strong Divergence (CSD) to converge to the right boundaries. The CSD are the points where the field changes direction. Even the generalized version (GGVF)[7] which is an improved one still could not handle these cases efficiently

Since we decide to extract the defects from the radiographic film background with parametric active contours, we had to choose a model that evolves quickly to the boundaries of the defect and fits even the narrow concavities. Moreover we need a model that is insensitive to the initialisation of the first contour. To deal with all these issues, we propose to join adaptive pressure forces to both the traditional gradient force, the GVF forces and even GGVF forces, in order to reduce their drawbacks and accelerate the motion of the resulting models. The new method is presented in detail in the following section

#### IV. DEFECTS DETECTION: FORCES ASSOCIATION FOR THE SNAKE MODEL

The pressure force has the attracting propriety of pushing any point of the curve forwards or backwards. One has just to choose the appropriate weight of the pressure force ( $k$ ). We propose to make the value and the sign of  $k$  changing adaptively with regard to the position of the snake node in the image, which makes the force inflating a part of the model if necessary while the other parts will be deflating automatically. This way, some parts of the curve will shrink while other parts of it expand. This reduces considerably the snake sensitivity to the initialization.

The main idea is to give the balloon force bigger weight when the snake node is far from the boundaries and drive it quickly to the edges. Moreover,  $k$  will go smaller in the latest stages, but still the pressure forces push the model to go even towards thin concavities when the traditional potential force or the GVF force becomes weak. In this way, the convergence speed is increased and the concavity tracking capacity is enhanced.

Let  $K$  be the matrix of all the pressure weights possible in the image. The simplest case of  $K$  is a distance map where every pixel in the image has a corresponding value representing its signed normalized and thresholded distance from an edge map first computed (positive inside the object to be detected for inflating and negative outside for deflating). To fixe a threshold for the distance map amounts to fixe the distances that exceed the threshold  $D_{MAX}$  to  $D_{MAX}$ . To normalize theses distances amounts that all distances will be included between 0 and et 1.

If an image pixel  $i$  is assigned the distance  $d_i$  then normalizing these distance means:

$$\forall i \dots d_i \leftarrow \frac{d_i}{D_{MAX}} \text{ where } D_{MAX} \text{ is the threshold}$$

The figures below illustrate examples of theses operations where a part of a distance map of an object is shown in Fig. 2.

The object boundaries are fixed to "0". These distances are thresholded (in Fig. 4) and then normalized in Fig. 5.

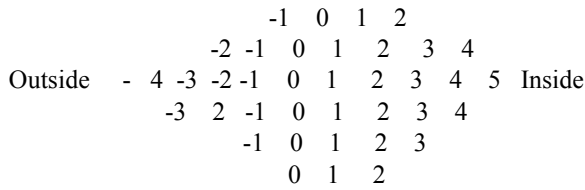


Fig. 3 a signed distance

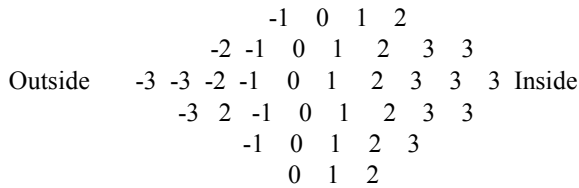


Fig. 4 the same distance thresholded to the distance 3

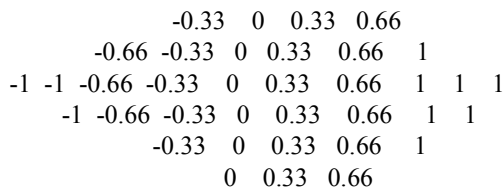


Fig. 5 After the normalization operation

Each snake node  $s$  will have as a pressure weight the product of the distance map value at the location of this node  $d(s, edge)$  and the value of a function at  $s$ ,  $\varphi(s)$ . The dynamics equation that governs this snake model is given:

$$I_t(s) = \alpha I''(s) + \beta I'(s) + (1 - \varphi(s))V + \varphi(s)d(s, edge)\vec{n}(s) \quad (6)$$

where  $V = (u, v)$  is the GVF vectors,  $d(s, edge)\vec{n}(s)$  the pressure force at the point  $s$ ,  $d(s, edge)$  the force weight and  $\varphi$  the inhibition function of the pressure forces near the boundaries and those of the GVF elsewhere. The inhibition function we choose is given by:

$$\varphi(s) = \exp\left(1 - \left(\frac{1}{d(s, contour)^p}\right)\right) \quad (7)$$

where  $p$  is an even scalar.

So thus,  $\varphi(s)$  tends to the value 1 when the snake nodes are far from the boundaries to be detected and be cancelled out near these boundaries and then and annul in the same time the pressure forces. In this way, the GVF and pressure force competition is eliminated. However to compute the distance map we need, we had to resort to a first coarse segmentation by thresholding. This can be summarized by the following flowchart

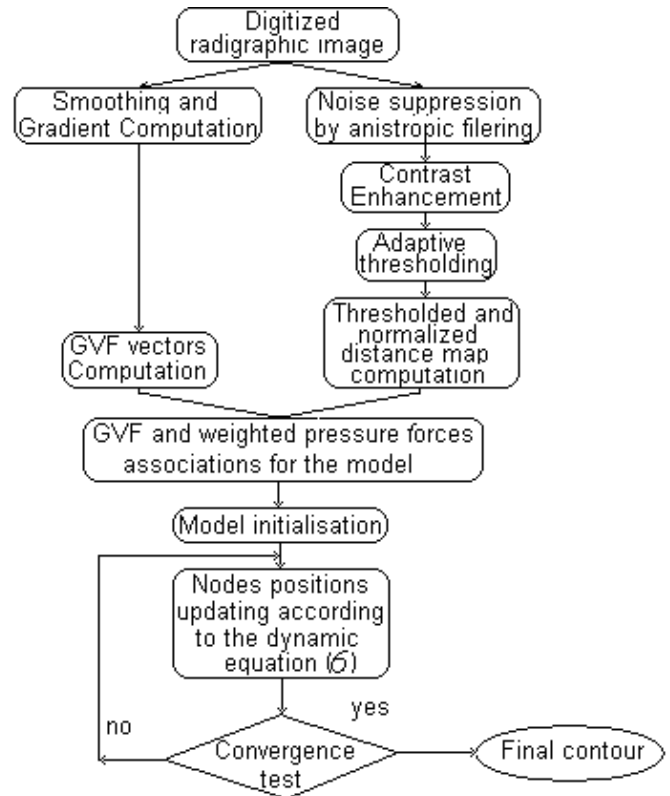
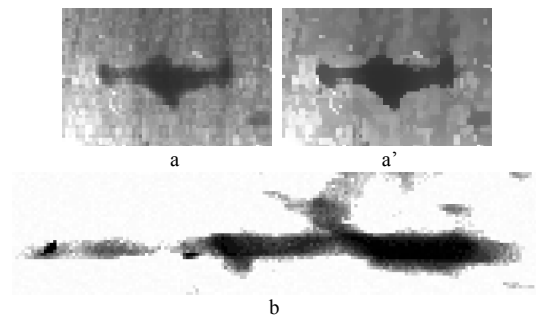


Fig. 6 The flowchart of the methodology

## V.RESULTS

As shown in the precedent section, the boundary extraction stage was preceded by a noise reduction and contrast enhancement stages to enhance the snake performance, and drive it to the real boundaries. Noise reduction was achieved by an edge preserving smoothing, while for the contrast enhancement; we tried a set of adaptive methods. The deduction we made about these methods is that the application of adaptive methods can alter the well contrasted and good quality images. So even these methods are a powerful tool to make visible the objects or a part of objects hidden by the low contrast or the non uniform illumination, they must be exploited carefully. In presence of a non-uniform illumination (see Fig.7 c'), the methods based on statistics and adaptive histogram equalization revealed to give the best results, otherwise, the morphological based methods seem to be sufficient to achieve a good contrast enhancement.



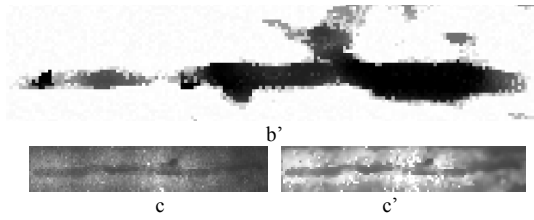


Fig. 7 An example of contrast enhancement, a', b' morphological methods and c' a statistics method

Moreover, thresholding was followed by some morphological filtering to get smooth boundaries. And example of the operations done before the distance map computation is given in Fig. 8

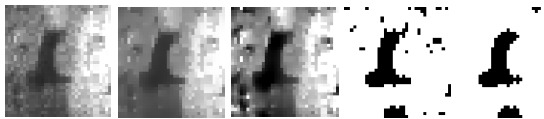


Fig. 8 An example of all the operations that precede the distance map computation, edge preserving smoothing, contrast enhancement, thresholding and morphological smoothing

First we tried the gradient, the GVF and also the GGVF [7] models on radiographic images for defect delineation. However the result was poor, as we have expected. The contour evolves till it collapse on the nearest edge of the defect as shown in the example of Fig. 9

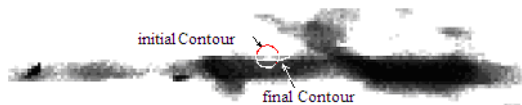
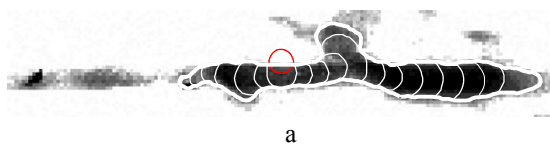
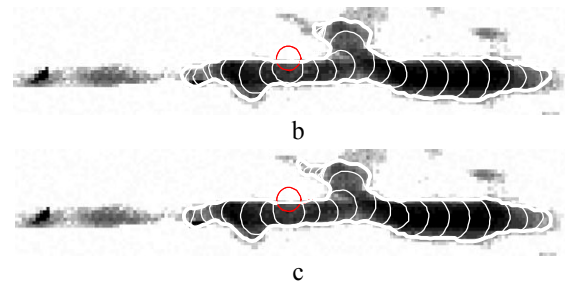


Fig. 9 initial and final contours for gradient GVF and GGVF models

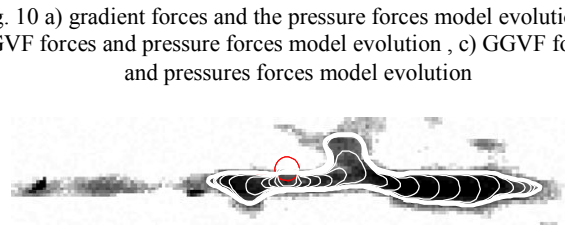
After we tried snakes where we have associated first the adaptive pressure force and the gradient forces then the adaptive pressure forces and the GVF ones, and at late the adaptive pressure forces and the GGVF forces. The results are shown below in Fig. 10 the Fig. 11 shows the behavior of the model with only the pressure forces, which guide the curve near the edge but can not achieve the evolution to fit the boundaries. That is why additional forces are required. So, the gradient, GVF and GGVF forces attract the curve to the boundaries, but the best result seems to be the one where the pressure forces are combined with the GGVF ones as shown in Fig. 10 .c. The four models had the same initialization but the final results are different with an advantage for the combination with the GGVF over the others. As a conclusion, in addition of less sensitivity to initialization, our model makes the snake evolving where the GVF and the GGVF snakes stagnate.



a



b



c

Fig. 10 a) gradient forces and the pressure forces model evolution, b) GVF forces and pressure forces model evolution, c) GGVF forces and pressures forces model evolution



Fig. 11 The model evolution only with the adaptive pressure forces

Below we show some examples of weld defect extraction from radiographic images with the association of adaptive pressure forces and the GGVF ones. The results show a successful contour estimation for both cases, with a simple initialization consisting of a little circle crossing a part of the defects. Despite the relatively complicated with their concavities and thin and aligned parts, the proposed snake has progressed from the initial contours, by getting closer to the real boundaries until fitting the defect shape in the last ones.

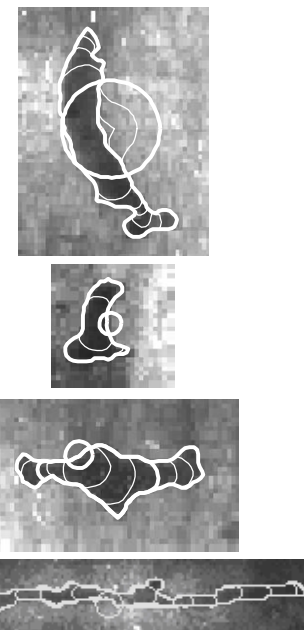


Fig. 12 The proposed model evolution (GGVF forces and weighted pressure one's combination to drive the model) from the initial contour represented as a circle crossing the defect to the final one

## VI. CONCLUSION

We have described an approach of boundaries extraction of weld defects in radiographic images, based on the combination of the well known GVF force and an adaptive pressure forces.

Experiments on real images have shown the ability of the proposed method to give a good estimation of the contours by fitting the concavities, and progressing where the GVF snake stagnates when used alone. Moreover, the snake has shown a less sensitivity to initialisation than the GVF and its improved version GGVF, and more progression speed even in thin concavities.

#### REFERENCES

- [1] Nockemann, C., Heidt, H., & Thomsen, N. (1991). Reliability in ndt: Roc study of radiographic weld inspections. *NDT and E International*, 24(5), 235–245.
- [2] N. Nacereddine, L. Hamami, D. Ziou, N. Tridi “Statistical tools for weld defect evaluation in radiographic testing” in *Proceeding of 9<sup>th</sup> European Conference on Non-Destructive Testing 2006*, Berlin, Germany, Sept. 25-29, 2006.
- [3] Nacereddine, N., Tridi, M.: Computer-Analysis and Classification of Welded industrial Radiography based Invariant Attributes Neural Networks. *Proceeding of the 4<sup>th</sup> Symposium on Image and Signal Processing Analysis, Zagreb, Croatia, (2005)* 88–93.
- [4] Kass, M., Witkin, A., Terzopoulos, D.: Snakes: Active Contour Models. *Int’l J. Computer Vision*, 321–331 (1988)
- [5] Caselles V, Catta F, Coll T, Dibos F. A geometric model for active contours in image processing. *Numer Math* 1993;66(1):1–31.
- [6] Xu C, Prince J. Snakes, shapes, and gradient vector flow. *IEEE Trans Image Process* 1998;7(3):359–69.
- [7] C. Xu and J. Prince, “Generalized Gradient Vector Flow: External Forces For active Contours”, *Signal Processing*, 1998, vol. 71, pp. 131-139.
- [8] Li C, Liu J, Fox MD. Segmentation of edge preserving gradient vector flow: an approach toward automatically initializing and splitting of snakes. In: *Proceedings of IEEE conference on computer vision and pattern recognition (CVPR)*, vol. 1. 2005. p. 162–7.
- [9] Ronfard R. Region-based strategies for active contour models. *Int J Comput Vis* 1994;13(2):229–51.
- [10] Ivins, J., Porrill, J.: Active region models for segmenting medical images. In: *Proceedings of the IEEE International Conference on Image Processing (1994)*
- [11] Abd-Almageed, W., Smith, C.E.: Mixture models for dynamic statistical pressure snakes. In: *IEEE International Conference on Pattern Recognition, Quebec City, Canada (2002)*
- [12] Abd-Almageed, W., Ramadan, S., Smith, C.E.: Kernel Snakes: Non-parametric Active Contour Models. In: *IEEE international conference on systems, man and cybernetics, Washington (2003)*
- [13] Chan T, Vese L. Active contours without edges. *IEEE Trans Image Process* 2001;10(2):266–77.
- [14] Paragios N, Deriche R. Geodesic active regions and level set methods for supervised texture segmentation. *Int J Comput Vis* 2002;46(3):223–47.
- [15] Jardim, S.M.G.V.B., Figuerido, M.A.T.: Segmentation of Fetal Ultrasound Images. *Ultrasound in Med. & Biol.* 31(2), 243–250 (2005)
- [16] A. B. Goumeidane, M. Khamadja, N. Nacereddine: Maximum Likelihood Curves for Multiple Objects Extraction: Application to Radiographic Inspection for Weld Defects Detection. *International Journal on New Computer Architectures and Their Applications (IJNCAA)* 1(4): 210-222
- [17] TIAN Yuan, DU Dong, CAI Guorui, WANG Li, ZHANG Hua: Automatic Defect Detection in X-Ray Images Using Image Data Fusion
- [18] P. Perona and J. Malik. “Scale-space and edge detection using anisotropic diffusion”, *IEEE trans. on Pattern Analysis and Machine Intelligence*, 12(7), July 1990.
- [19] F. Preteux, Description et interprétation des images par la morphologie mathématique. Application à l’imagerie médicale. Thèse d’état d l’université P. et M. Curie Paris VI. (1987) .
- [20] T. Stojić, I. Reljin, B. Rejlin, “Local Contrast Enhancement In Digital Mammography by using Mathematical Morphology” *IEEE Conference on 2005*.
- [21] I. El Feghi, S. Huang, M.A. Sid-Ahmed and M. Ahmadi , “Contrast enhancement of radiograph image based on local heterogeneity measures,” *ICIP 2004*.
- [22] Z. Tu and C. Bajai, “A Fast Adaptive Method for Image Contrast Enhancement”, *ICIP 2004*.
- [23] J. Kim, L. Kim, and S. Hwang, “An Advanced Contrast Enhancement Using Partially Overlapped Sub-Block Histogram Equalization,” *IEEE Trans. Circuit and systems* VOL. 11, NO. 4, APRIL 2001.
- [24] L. D. Cohen, “On active contour models and balloons,” *CVGIF: Image Understand.*, vol. 53, pp. 211 218, Mar. 1991.
- [25] L. D. Cohen and I. Cohen, “Finite-element methods for active contour models and balloons for 2-D and 3-D images,” *IEEE Trans. Pattern Anal. Machine Intell.*